SLAC–PUB–7899
July 1998

Wake Fields in a mm-Wave Linac*

F. Zimmermann, D.H. Whittum, C.K. Ng
Stanford Linear Accelerator Center
Stanford University, Stanford, CA 94309, USA

M.E. Hill†
Harvard University, Cambridge, MA 02138, USA

We estimate the short-range wake fields in the W-band active matrix linac of a 5-TeV collider, and demonstrate that for the assumed 60-pC bunch charge and 10-μm rms bunch length they are acceptable.

Presented at the
8th Workshop on Advanced Accelerator Concepts
Baltimore, Maryland, July 5–11, 1998

*Work supported by the U.S. Department of Energy, contract DE–AC03–76SF00515.
†Work supported under a National Science Foundation Graduate Fellowship.

Wake Fields in a mm-Wave Linac[1]

F. Zimmermann, D.H. Whittum, C.K. Ng and M.E. Hill † [2]

Stanford Linear Accelerator Center
Stanford University, Stanford California 94309

† *Harvard University, Cambridge, MA 02138*

Abstract. We estimate the short-range wake fields in the W-band active matrix linac of a 5-TeV collider, and demonstrate that for the assumed 60-pC bunch charge and 10-μm rms bunch length they are acceptable.

INTRODUCTION

We consider an active matrix linac as described in Ref. [1,2], operating at at a wavelength of $\lambda = 3.28$ mm (91 GHz). A single cavity of such an accelerator is sketched in Fig. 1. Viewed in the beam direction, the transverse dimension of the cavity is square with a full width of $\lambda/\sqrt{2}$ or a half width of $b = 1.16$ mm. The full cavity gap is $g = 0.37\lambda = 1.21$ mm, and the iris radius $a = 0.1\ \lambda = 0.328$ mm. We assume that the full period l is 25% larger than g, or $l = 1.51$ mm. The bunch charge is 60 pC (3.75×10^{10} electrons per bunch) and the rms bunch length is taken to be 10 μm. Cavity and beam parameters are summarized in Table 1. The calculations presented in this paper do not pay attention to the rectangular geometry of the cells. This is justified, since the irises are round and we are only concerned with the short-range wake fields.

LONGITUDINAL WAKE FIELD

Geometric Wake

The longitudinal geometric wake field is maximum at the position of the drive particle, where it assumes the value [3]

$$W_L(0) = \frac{Z_0 c}{\pi a^2} \tag{1}$$

[2] Work supported under a National Science Foundation Graduate Fellowship.
[1] Work supported by the U.S. Department of Energy under contract DE-AC03-76SF00515.

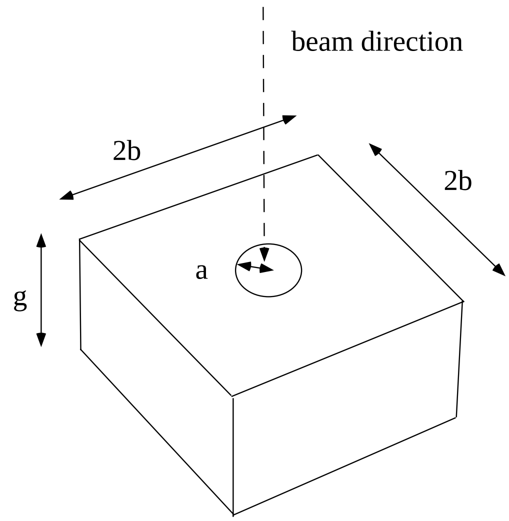

FIGURE 1. Schematic of a single cavity in a 2.5-GeV active matrix linac [1,2]

.

TABLE 1. Single-cell and beam parameters for the linac of a 5-TeV collider [1,2].

variable	symbol	value
charge per bunch	Q	60 pC
rms bunch length	σ_z	10 μm
wavelength	λ	3.28 mm
full gap	g	1.21 mm
iris radius	a	0.328 mm
full period	l	1.51 mm
cavity half width	b	1.16 mm

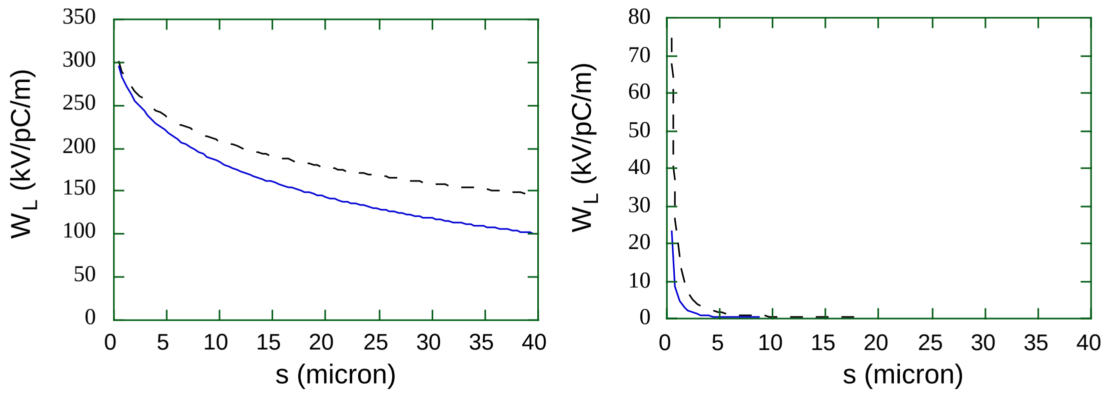

FIGURE 2. Left: longitudinal geometric wake field vs. distance for $a/\lambda = 0.1$; dashed: Eq. (2), solid: Eq. (3). Right: longitudinal resistive-wall wake field vs. distance; dashed: cavity walls, solid: iris.

with $Z_0 = 377\ \Omega$. Thus $W_L(0)$ depends only on the iris radius of the cavity. For our cell, it evaluates to 336 kV/pC/m. As a worst case, we could assume that the wake field is constant across the bunch, equal to $W_L(0)$. If we then consider a beam of charge Q equal to 60 pC, the induced voltage is 20 MV/m, a factor 50 smaller than the accelerating gradient of 1 GV/m.

Let us now include the s-dependence of the short-range wake field. An inverse Fourier transform of the high-frequency impedance derived in Ref. [3] yields [4]

$$W_L(s) \approx \frac{Z_0 c}{\pi a^2} \exp\left(\frac{2\pi\alpha^2 l^2 s}{a^2 g}\right)\ \mathrm{erfc}\left(\frac{\alpha l}{a}\sqrt{\frac{2\pi s}{g}}\right) \tag{2}$$

where, for $g/l \to 1$, the coefficient α approaches 0.46 [4].

In Ref. [4] an alternative approximation to the short-range wake field was given: Over a wide parameter range, the wake fields from a complex-frequency domain calculation are well reproduced by a quasi-exponential decay [4],

$$W_L(s) = \frac{Z_0 c}{\pi a^2}\ \exp\left(-\sqrt{s/s_e}\right) \tag{3}$$

where

$$s_e = 0.41\ \frac{a^{1.8} g^{1.6}}{l^{2.4}} \tag{4}$$

is the decay length. In our example, $s_e \approx 27\ \mu$m.

Equations (2) and (3), evaluated for the parameters of Table 1, are plotted in Fig. 2 (left). The two curves are quite different at large s. Based on the results of Ref. [4], we expect that Eq. (3) provides the more accurate description.

Resistive-Wall Wake

The character of the resistive wall wake field is determined by the ratio between bunch length and the characteristic distance [5]

$$s_0 = \left(\frac{cb_p^2}{2\pi\sigma}\right)^{1/3} \tag{5}$$

where σ denotes the conductivity in cgs units (for copper at room temperature $\sigma = 5.8 \times 10^{17}$ s^{-1}) and b_p is radius of the beam pipe. In this case b_p is either equal to iris radius a or the cavity half width b, for which $s_0 \approx 2$ μm and $s_0 \approx 5$ μm, respectively. The bunch length $\sigma_z \approx 10$ μm is a factor 2–5 larger than s_0. Hence we can, in a good approximation, use the formula for the resistive-wall wake field of a long bunch, derived by Chao [6]:

$$W_L(s) = \frac{Z_0 c}{2(2\pi)^{3/2} b_p^2} \left(\frac{s_0}{s}\right)^{3/2} \tag{6}$$

Since the iris walls occupy about 20% of the total length, and their radius a is about 1/3 of b, we find that the contributions to the resistive-wall wake field from iris and cavity wall are comparable.

These two wake fields, for iris and walls, are depicted in Fig. 2 (right), where we have multiplied by the different filling factors of about 20% and 80%, respectively. The resistive wake field falls off rapidly over a distance much shorter than the bunch length, and its magnitude is small compared with the geometric wake. Thus, the longitudinal resistive-wall wake field can be neglected.

Coating and Surface Roughness

The effects of a dielectric coating or surface roughness can be described by [8]:

$$W_L(s) = \frac{Z_0 c}{\pi b_p^2} \cos k_0 s \tag{7}$$

where

$$k_0 = \left(\frac{2\epsilon}{b_p \delta(\epsilon - 1)}\right)^{1/2}, \tag{8}$$

b_p is the radius of the beam pipe (*e.g.*, equal to b or a), and δ the thickness of the dieletric layer or corrugation.

It is foreseen as an option to coat the inside of the W-band cells with a 5-μm layer of diamond ($\epsilon = 5.5$) [7]. According to a recipe put forward in Ref. [8], to describe the effect of surface roughness we should use Eqs. (7) and (8) with $\epsilon \approx 2$. Using $b_p = b$, we then find, $1/k_0^{(1)} \approx 49$ μm for the dielectric, and $1/k_0^{(2)} \approx 17$ μm for a pessimistic 1-μm surface roughness. The corresponding wake functions are shown in Fig. 3. They are comparable to the geometric wake field.

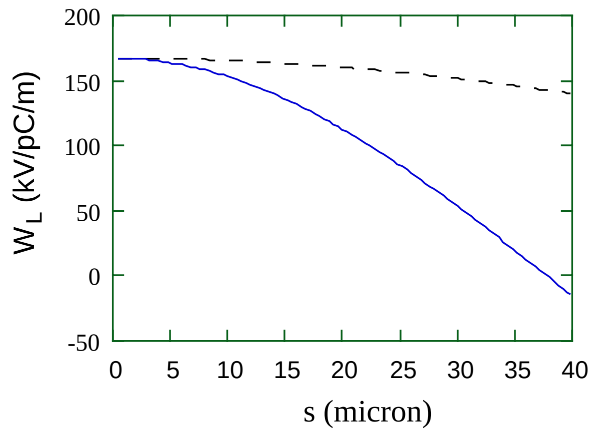

FIGURE 3. Longitudinal wake field for a 5 μm diamond coating (dashed) and a 1 μm surface roughness (solid) vs. distance.

Total Longitudinal Wake

The total wake is now the sum of the geometric, the dielectric and the surface roughness wakes (we neglect the resistive-wall wake field, since it is much smaller). If we fold the Green function wake $W_L(s)$ with a (Gaussian) charge distribution, we obtain the beam-induced voltage for the entire bunch:

$$V_L(s) = \frac{Ne}{\sqrt{2\pi}\sigma_z} \int_{-\infty}^{s} W_L(s - s') e^{-\frac{s'^2}{2\sigma_z^2}} \, ds' \tag{9}$$

with

$$W_L(s) \approx \frac{Z_0 c}{\pi} \left(\frac{e^{-\sqrt{s/s_e}}}{a^2} + \frac{\cos k_0^{(1)} s}{b^2} + \frac{\cos k_0^{(2)} s}{b^2} \right) \tag{10}$$

In Fig. 4 (left) we compare the total beam induced voltage, the bunch wake field without dielectric coating and the geometric wake field alone, all obtained by numerical integration of Eq. (9). For the latter case, we also present the result of a MAFIA calculation, which is in reasonable agreement, and thus confirms the approximation of Eq. (3). As can be seen, the dielectric and roughness components contribute a little more than half the total.

Figure 4 (right) shows the beam-induced voltage V_L at a distance σ_z behind the bunch center, due to the geometric wake field only, vs. the ratio a/λ. In calculating V_L we have used the fit result of Eq. (3). This figure demonstrates that opening the iris radius from 0.1λ to 0.17λ would decrease V_L by about a factor of 3.

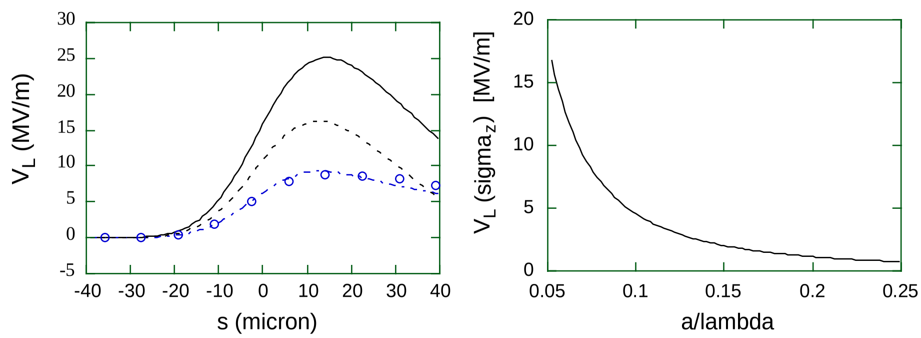

FIGURE 4. Left: beam-induced voltage V_L vs. distance from the bunch center, for a Gaussian bunch with 60 pC charge and 10 μm rms length, and $a/\lambda = 0.1$. The total voltage arising from geometric, dielectric and roughness wake fields (solid) is compared with the induced voltage without dielectric (dashed) and that due to the geometric wake field only, using the approximation of Eq. (3) (dot-dashed) and calculated by MAFIA (the circles). Right: beam-induced voltage $V_L(\sigma_z)$ due to the geometric wake field only as a function of a/λ, according to Eq. (3), again for a Gaussian bunch with 60 pC charge and 10 μm rms length.

TRANSVERSE WAKE FIELD

Resistive Wall

The transverse effect of the wall resistivity is described by the wake function[3] [6]

$$W_T(s) = \frac{Z_0 c}{4\pi^2 b_p^3}\sqrt{\frac{c}{\sigma}}\,\frac{1}{\sqrt{s}}, \tag{11}$$

where as for the longitudinal case σ denotes the conductivity in cgs units (for copper at room temperature $\sigma = 5.8 \times 10^{17}\ \mathrm{s}^{-1}$) and b_p is the radius of the beam pipe. This formula applies for distances s larger than $(c/(4\pi\sigma b_p))^{1/3} b_p$, which amounts to 1.6 μm for the iris, and 3.8 μm for the cavity walls. The resistive-wall transverse wake fields due to iris and wall are illustrated in Fig. 5.

Geometric Wake

The slope of the transverse geometric wake field at the origin is determined by the iris radius [9]:

$$W_T'(0) = \frac{2 Z_0 c}{\pi a^4} \tag{12}$$

and evaluates to 6 $\mathrm{TV/m^3/pC}$, or, in Gaussian units, to $7 \times 10^6\ \mathrm{cm}^{-4}$. At higher frequencies, the impedance can be derived from a diffraction model and decays as

[3] We here adopt a sign convention opposite to that in Ref. [6].

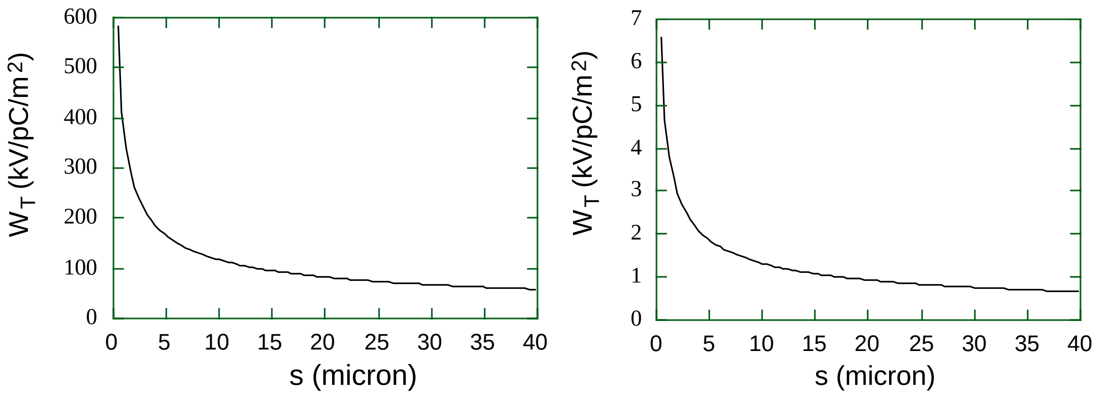

FIGURE 5. Transverse resistive wall wake field vs. distance; left: contribution from iris; right: contribution from cavity wall.

$\omega^{-3/2}$ [10]. However, no general formula exists for the low-frequency part of the impedance, and, to compute the wake field, we resort to a numerical calculation using MAFIA [11]. As the bunch passes through a periodic array of cells, the wake field reaches a steady state after about [12] $n_{crit} \approx a^2/(4\sqrt{3}g\sigma_z)$ number of cells. In our case, $n_{crit} \approx 1$. Using MAFIA we calculated the wake fields for an array of 4 and for 3 cells, and took the difference to obtain an estimate of the steady state wake field per cell.

The result of this calculation for a 10 μm rms bunch length and $a/\lambda = 0.1$ is shown in Fig. 6 (left), where it is also compared with the bunch wake field

$$V_T(s) = \frac{Ne}{\sqrt{2\pi}\sigma_z} \int_{-\infty}^{s} (s - s')\; W_T'(0) e^{-\frac{s'^2}{2\sigma_z^2}}\; ds', \tag{13}$$

expected for a purely linear wake with slope given by Eq. (12). Figure 6 (right) shows the bunch wake field $V_T(s)$, for three different values of a/λ, as calculated by MAFIA. From these curves, we can deduce the effective slope W_T'. For $a/\lambda = 0.1$ this slope is about 2.5 TV/m^3/pC, or, in Gaussian units, 3×10^6 cm^{-4}, and thus a factor 2–3 smaller than the point-bunch slope. For $a/\lambda = 0.15$ the effective slope is about 0.7 TV/m^3/pC, or 8×10^5 cm^{-4}, and for $a/\lambda = 0.2$ it is 0.25 TV/m^3/pC, or 3×10^5 cm^{-4}.

Coating and Surface Roughness

The longitudinal impedance corresponding to the wake function of Eq. (7) is

$$Z_L(k) = \int_0^{\infty} ds\; W_L(s) e^{iks} = \frac{Z_0 c}{\pi 2b^2}\; [\delta(k - k_0) + \delta(k + k_0)] \tag{14}$$

The transverse impedance of a small perturbation is related to the longitudinal impedance via [6] $Z_T(k) = 2Z_L(k)/(kb^2)$, so that

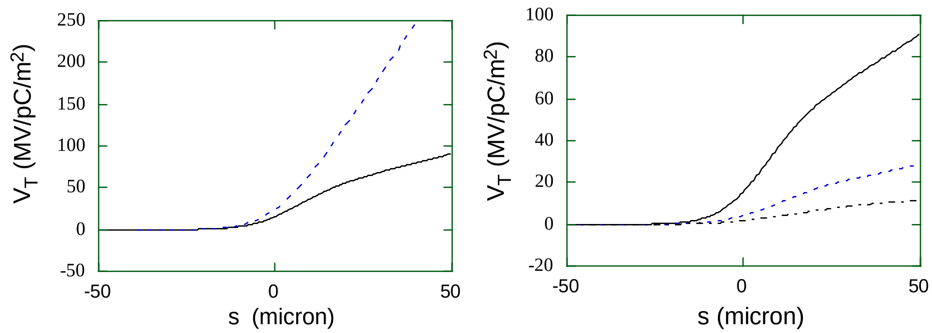

FIGURE 6. Transverse geometric wake field $V_T(s)$ for a 10 μm rms bunch length vs. distance s. Left: wake field for $a/\lambda = 0.1$, according to a MAFIA calculation (solid), and for a simplified linear wake (dashed) with slope as in Eq. (12). Right: geometric wake field calculated by MAFIA for a 10 μm rms bunch length, considering $a/\lambda = 0.1$ (solid), 0.15 (dashed) and 0.2 (dot-dashed).

$$Z_T(k) = \frac{cZ_0}{kb^4}\left[\frac{\delta(k-k_0)+\delta(k+k_0)}{k}\right] \tag{15}$$

We obtain the transverse wake field by Fourier transform

$$W_T(s) = \frac{i}{2\pi}\int_{-\infty}^{\infty} dk\ Z_T(k)e^{-iks} = \frac{Z_0 c}{\pi b^4}\left[\frac{\sin k_0 s}{k_0}\right] \tag{16}$$

Its slope at the origin is $W_T'(0) = \frac{2Z_0c}{\pi b^4}$, independent of k_0, and this evaluates to 40 GV/m^3/pC or, in Gaussian units, to 4×10^4 cm^{-4}.

Beam Break Up

Single bunch charge in the W-band linac is constrained by beam break up. The motion of a beam-slice centroid takes the form $x(s,z) = \mathrm{Re}(\chi(s,z)B(s))$, where $B = (\beta/\gamma)^{1/2}e^{j\psi}$ describes the machine lattice in terms of the beta function β, Lorentz factor γ and betatron phase ψ. The coordinate s is the position along the linac, and z is the longitudinal distance from the bunch head. The asymptotic solution for a unit initial offset in the presence of a linear (in z) wake field is [13,14]

$$\chi \approx \frac{3^{1/4}}{2^{3/2}\pi^{1/2}}\ \frac{1}{A^{1/2}}\exp\left\{A\left(1-\frac{j}{3^{1/2}}\right)+j\frac{\pi}{12}\right\} \tag{17}$$

where, for a lattice with $\beta \propto \sqrt{\gamma}$,

$$A = \frac{3^{3/2}}{2^{5/3}}\left(\frac{\beta_0}{GL^2}\right)^{1/3}\left(\sqrt{\frac{\gamma}{\gamma_0}}-1\right)^{1/3}. \tag{18}$$

The characteristic length L is related to the strength of the wake field,

$$L = \left(\frac{e^2 N_b W_T'(0) l_b}{mc^2} \right)^{-1/2}, \tag{19}$$

where l_b is the (flat-top) bunch length, taken to be 30 μm, and r_e the classical electron radius. The largest transverse wake is the geometric one. The left picture of Fig. 7 shows the variation of L as a function of a/λ, inferred from the effective slope $W_T'(0)$ provided by MAFIA. The characteristic length L is 1 cm for $a/\lambda = 0.1$, and about 3.5 cm for $a/\lambda = 0.2$.

Figure 7 (right) compares the analytical solutions of the oscillation growth for L equal to 1 and 3 cm with the result of a macroparticle simulation, where we have assumed an initial beta function $\beta_0 \approx 1.6$ m at 10 GeV, increasing along the linac as $\gamma^{1/2}$, an accelerating gradient of $G \approx 1$ GV/m, and 60 pC bunch charge. With $L \approx 1$ cm, an initial offset gets amplified by more than a factor of 10. For $L > 3$ cm, there is negligible growth in the linac, and this value of L would be obtained for $a/\lambda \geq 0.18$.

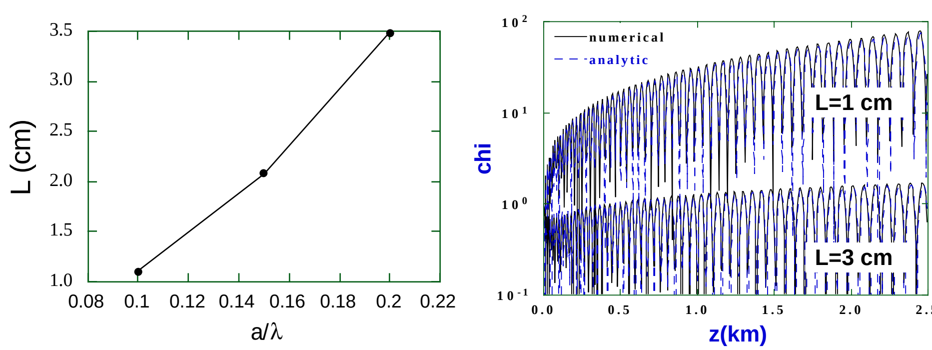

FIGURE 7. Left: the characteristic length L, inferred from MAFIA calculations, for an rms bunch length of 10 μm and a 60 pC charge as a function of a/λ. Right: simulated and analytical beam break up for two different values of L, without BNS damping.

CONCLUSION

We have estimated the longitudinal and transverse wake fields in a W-band (91 GHz) accelerating structure. The transverse wake field is almost completely determined by the structure geometry (iris radius). For a 60 pC charge, and $a/\lambda \geq 0.18$, the transverse beam break up is negligible. In the longitudinal plane, the effect of a dieletric coating and of surface roughness could become as significant as the geometric wake field. The single-bunch beam loading due to the geometric wake field is much less than 1% of the accelerating gradient. The resistive-wall wake fields are insignificant in all cases.

REFERENCES

1. D.H. Whittum and S.G. Tantawi, "Active Millimeter Wave Accelerator with Parallel Beams", *SLAC-PUB*-**7845** (1998).
2. D. Whittum, these proceedings.
3. R. Gluckstern, *Phys. Rev. D* **39**, p. 960 (1989).
4. K.L.F. Bane, A. Mosnier, A. Novokhatskii, K. Yokoya, "Calculations of the Short-Range Longitudinal Wake Fields in the NLC linac", presented at EPAC98, Stockholm, and *SLAC-PUB*-**7862** (1998).
5. K.L.F. Bane and M. Sands, "The Short-Range Resistive Wall Wake Fields", in *Micro Bunches Workshop*, Upton, *AIP Conference Proceedings* **367** (1995).
6. A.W. Chao, "Physics of Collective Beam Instabilities in High Energy Accelerators", John Wiley & Sons, Inc., New York (1993).
7. E. Lin, private communication (1998).
8. A. Novokhatskii and A. Mosnier, "Wake Fields of Short Bunches in the Canal Covered with Thin Dieletric Layer".
9. K. Bane, in chapter 8 of the "Zeroth Order Design Report for the Next Linear Collider", *SLAC Report* **474**, p. 368 (1996).
10. S.A. Heifets and S.A. Kheifets, "Coupling Impedance in Modern Accelerators", *Rev. Mod. Physics*, **63**, 631 (1991).
11. "MAFIA RELEASE 3", *DESY* **M-90-05K** (1990).
12. R. Palmer, "Radiation from a Ring Charge Passing Through a Resonator", *Particle Accelerators*, **25**, p. 107 (1990).
13. F. Zimmermann, D.H. Whittum and M.E. Hill, "New Concepts for a Compact 5 TeV Collider", presented at the *6th European Particle Accelerator Conference (EPAC 98)*, Stockholm, and *SLAC-PUB*-**7856** (1998).
14. D.H. Whittum, M.E. Hill and F. Zimmermann, "Transverse Beam Dynamics in a mm-Wave Planar Accelerator", unpublished.
15. F. Zimmermann and D.H. Whittum, "Final-Focus System and Collision Schemes for a 5-TeV W-Band Linear Collider", *Proc. of 2nd Int. Workshop on e^-e^- Interactions at TeV Energies*, Santa Cruz 1997 and *SLAC-PUB*-**7741**(1998).